The Drop-Size Response of the CSIRO Liquid Water Probe

C. J. BITER

The National Center for Atmospheric Research, Boulder, CO 80307*

J. E. DYE

The National Center for Atmospheric Research, Boulder, CO 80307*

D. HUFFMAN

Particle Measuring Systems, Boulder, CO 80302

W. D. KING

CSIRO, Melbourne, Australia

(Manuscript received 31 January 1986, in final form 12 November 1986)

ABSTRACT

The response of the CSIRO liquid water content (LWC) device to water drops of different sizes has been investigated in a wind tunnel. Two series of experiments were conducted. The first compared the probe-measured LWC of sprays with different median volume diameters (MVD) to the LWC computed through water mass conservation considerations; the second series compared the probe LWC to that computed from the droplet spectra measured by Particle Measuring Systems' (PMS) probes. In the first series of experiments, the response was found to decrease from 100% for a water spray with an MVD of ~20 μm to about 50% for a spray with an MVD of ~150–200 μm. From these results, we expect that the King Probe can be used without correction for measuring the LWC of droplet distributions with MVDs less than about 40 μm. As the MVD increases, there will be a gradually diminishing response, which for MVDs of greater than 100 μm will require substantial correction.

The second series of experiments produced physically unreasonable results, suggesting that the size calibration of the PMS Forward Scattering Spectrometer Probe needs to be reevaluated. These results also indicate that a correction is required for the PMS Two-Dimensional Grey Optical Array Imaging Probe.

1. Introduction

The most widely used sensors for directly measuring the liquid water content (LWC) of clouds today are the Johnson–Williams hot wire, commonly called the J–W, and the Commonwealth Scientific and Industrial Research Organization (CSIRO) constant-temperature, hot wire. Since this second device is often called the "King Probe," we will hereafter refer to it as the KP.

Measurements from both of these probes are sensitive to the size of the water drops encountered. It has been known for some time that the J–W underestimates the mass of droplets with diameters greater than about 30 μm and has virtually no response to precipitation-size drops (Owens, 1957; Barrett, 1958; Knollenberg, 1972). While recent tests on the KP (King et al., 1985) suggest that it has nearly 100% response to drops of about 20-μm diameter over a wide range of environmental conditions, there is little or no documentation of its response to larger drops. King (1982) has shown that there are occasions where it can overread liquid water contents derived from the Forward Scattering Spectrometer Probe (FSSP) by a factor of two, and that these situations are generally related to the presence of drops in excess of 47 μm diameter, the upper limit of the FSSP. Strapp (personal communication) has also collected data showing that its response to millimetric-size drops is not negligible, so there is some evidence that the roll-off in response occurs at larger drop sizes than the J–W probe. This, of course, is not entirely unexpected in view of the relative diameters for the two probes: 0.53 mm for the J–W and approximately 2 mm for the KP. For many applications it is important to be able to specify the roll-off characteristics since the partition of the total LWC into cloud water, drizzle water, and rain water components is an important consideration for the formation of precipitation.

This paper reports on two types of wind tunnel experiments that were conducted to determine the response of the KP as a function of drop size. In the first

*The National Center for Atmospheric Research is funded by the National Science Foundation.

© 1987 American Meteorological Society

Unauthenticated | Downloaded 06/07/23 02:35 AM UTC

series of experiments, the KP response was compared with values of liquid water content calculated on the basis of conservation of the mass of water in the tunnel. The second series of experiments used the Particle Measuring Systems' (PMS) FSSP and a 64-element 2D Grey Optical Array Imaging Probe (hereafter referred to as the 2D-GA) to measure the droplet spectrum from which the LWC was computed. The central theme of this paper is the resulting KP response curve. Also presented is compelling, albeit circumstantial, evidence obtained during the experiments that indicates that the recommended drop-size calibration procedures for the FSSP need to be reevaluated. Some correction may also be required for the 2D-GA probe.

2. The wind tunnel

The experiments were performed in the Particle Measuring Systems' (PMS) low-speed, open-circuit wind tunnel at their Boulder, Colorado facility. Figure 1 shows the tunnel test section and several salient features of the experimental set up. The test section is 3 m long by 0.76 m in diameter. Airspeed can be varied up to about 100 m s^{-1} and is measured by a propeller anemometer. Critical absolute velocity measurement was not essential to the experiments described herein since each of the LWC measuring techniques is sensitive to particle flux rather than absolute concentrations. Nevertheless, a pitot tube was used to verify the anemometer calibration and to obtain a velocity profile across the test section. No speed difference could be detected over the measurable region (farther than 4 cm from the tunnel walls due to pitot construction).

Water spray was injected through a single nozzle located 94 cm upstream of the instrument sample area. A single nozzle at this location produced more consistent spray patterns with narrower drop-size distributions than could be obtained by using multiple identical nozzles located in existing spray rigs in the tunnel contraction section. Two types of nozzles were used. An atomizing nozzle, in which both air and water were pumped into the nozzle under pressure, produced small-droplet sprays with median volume diameters (MVD) in the range of 15 to 20 μm. Larger-droplet sprays with MVDs of 33 to 270 μm were achieved using three different hydraulic (water only) nozzles. For a given hydraulic nozzle, variations in MVD could be produced by altering the hydraulic pressure.

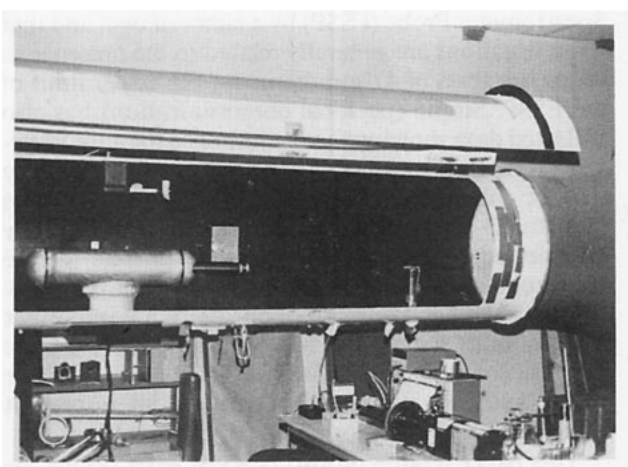

FIG. 1. The wind tunnel test section instrumented with propeller anemometer, FSSP, and single hydraulic nozzle.

Regulated air pressure (up to 21 kPa) was supplied to a water-filled pressure vessel, in parallel to the air atomizing nozzle when it was used. Water flow rates from the pressure vessel to the nozzle were adjustable through a needle valve assembly and were monitored with a rotameter. Nozzle flow rates were calibrated by collecting and weighing the water output for given water and air pressures, water temperature, and flow-rate conditions. Even with the above techniques, the LWC and MVD could not be controlled independently.

Since the PMS tunnel is open to the atmosphere at both ends there was no effective control of air temperature, pressure, and relative humidity. Operating conditions were as follows: pressure ranged from 82–84 kPa, temperature from 4–26°C, and relative humidity from 22–86%. Airspeed was maintained at 60 m s^{-1} for all tests described here. Although we had hoped to perform tests at higher aircraft speeds, we were not able to because of limitations of the spray pattern at the higher speeds.

3. Analysis of the King Probe data

All of the tests were conducted with a short probe, identical to the one labeled PMS-USA in King et al. (1985), and contains all the modifications recommended therein. This version is commercially produced by PMS. The dimensions of the master coil in the sensor head were 1.79-mm diameter by 20.0-mm length. For these experiments, which were performed at above freezing temperatures, the tip heaters were removed and the aerodynamically faired tip covers were replaced with short caps that enabled the KP to be used either by itself or mounted inside the arms of the 2D-GA as shown in Fig. 2. Tests were conducted to determine if the use of the modified tip covers or the placement of the KP within the arms of the 2D-GA resulted in errors in the measured LWC relative to the standard probe configuration. No differences could be detected.

In the tunnel tests, the amount of power required to balance the forced convective heat loss from the KP sensor in dry operating conditions was determined with the tunnel at operating speed and the nozzle water turned off. Water was then forced through the nozzle and the LWC was calculated from the incremental power. The KP output was recorded on a chart recorder, and averaged for a 30-s period after steady conditions had been achieved. In the conversion from dis-

Unauthenticated | Downloaded 06/07/23 02:35 AM UTC

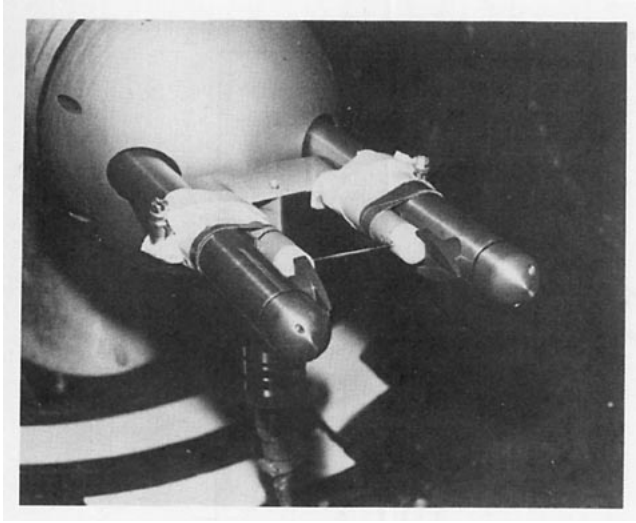

FIG. 2. The King probe mounted inside the "arms" of the 2D-GA. This mounting configuration was used during the second series of experiments.

sipated power to calculated LWC, allowances for collision efficiencies, etc. were carried out in an identical fashion to that described in King et al. (1985).

4. Measurements of the drop-size distribution

The drop-size distribution at the sample location was determined using the FSSP probe operating in the 2–47 μm range and the 64-element, 2D-GA probe operating with 15-μm resolution through the range of $\sim$10 to 938 μm. Two different FSSPs, one of which was subsequently found to be seriously undercounting, were used throughout most of the experiments and a third FSSP was used for a short time-period to help resolve the undercounting problem. Depths-of-field and beam diameters for the probes were determined in the manner described by Dye and Baumgardner (1984). The electronic particle counting circuits were checked by exciting the FSSP signal photodiode detector with a flashing diode device. It is noteworthy that the undercounting unit showed no anomalous behavior during any of these calibrations and tests. After a lengthy series of comparative wind tunnel and electronic bench tests, the undercounting probe was found to be operating in a retriggerable mode (see Cooper, 1978) even though it was thought that it had been modified for nonretriggerable operations.

Coincidence errors for the retriggerable probe have been corrected in accordance with Cooper (1978). Coincidence errors for the other two probes have been allowed for according to the technique given by Baumgardner et al. (1985). Using the worst-case conditions encountered during the tests (actual concentrations of $\sim$640 cm^3), these corrections amounted to 240% for the retriggerable probe and 11% for the nonretriggerable probes, while corrections for typical conditions (concentrations of $\sim$100 cm^{-3}) amounted to 16% and 3%, respectively. With corrections applied, the computed LWCs from each probe are within $\pm$20% of the average value of the three probes for a given set of operating conditions, including the worst case.

Glass beads were used to calibrate the first two FSSPs on the 2–47 μm range. Figure 3 shows the calibration points for these probes—serial numbers 20 and 72—superimposed on Fig. 9a from Dye and Baumgardner (1984), which shows similar calibration points (using the same glass beads) for seven other sensors calibrated on the 2–31-μm range. All points are corrected for the index of refraction of water based on theoretical scattering cross sections (Cerni, 1983) corresponding to the scattering angles of acceptance of each probe. The least-squares linear fit line to the glass bead data for all nine instruments (eight FSSPs and one ASSP) differs substantially from the manufacturer's calibration depicted by the 1:1 line. As pointed out by Dye and Baumgardner, the bead data suggest that the probes oversize small drops ($\leqslant$11 μm) and undersize larger ones ($\geqslant$11 μm). Both calibrations have been used in the reduction of the FSSP data; the significance of their difference is discussed later. A recording system malfunction precluded calibrating the third FSSP with glass beads. The preceding calibrations have been assumed in reducing the data from this last probe and the validity of this assumption is supported by measurements in the tunnel which show the modal diameters for a given spray condition to be comparable to those measured by the other FSSPs.

Data from the 2D-GA probe were processed and recorded on cassette by a PMS Particle Data Processing System (PDPS-11C). Each particle was subjected to minimum size, edge reject, and depth-of-field criteria prior to recording, and was sized using the midgrey (50%) shadow level as in nongrey probes. The edge-reject criteria ensured that only data from particles whose images were completely contained within the photodiode array (i.e., an edge element was not obscured) were recorded. As a result, the effective sample width decreases with increasing size. The probe sample area was also varied as a function of particle size in accordance with variations in the depth of field given by Knollenberg (1970). Particles that arrived while a valid particle was being processed were counted and added to the total count for the size bin of the processed particle. Glass beads dropped through the 2D-GA verified the manufacturer's calibration.

The total droplet spectrum was then obtained by combining the FSSP and 2D-GA data. CALIB1 will be used to refer to the spectra obtained by using the manufacturer's calibrations, without modifications, to reduce both FSSP and 2D-GA data. The spectrum in this case covers the range of 2–938 μm and is formed by combining channels 1–13 from the FSSP, with channels 3–62 from the 2D-GA resulting in a slight overlap of data for a 0.6-μm region at the juncture.

Unauthenticated | Downloaded 06/07/23 02:35 AM UTC

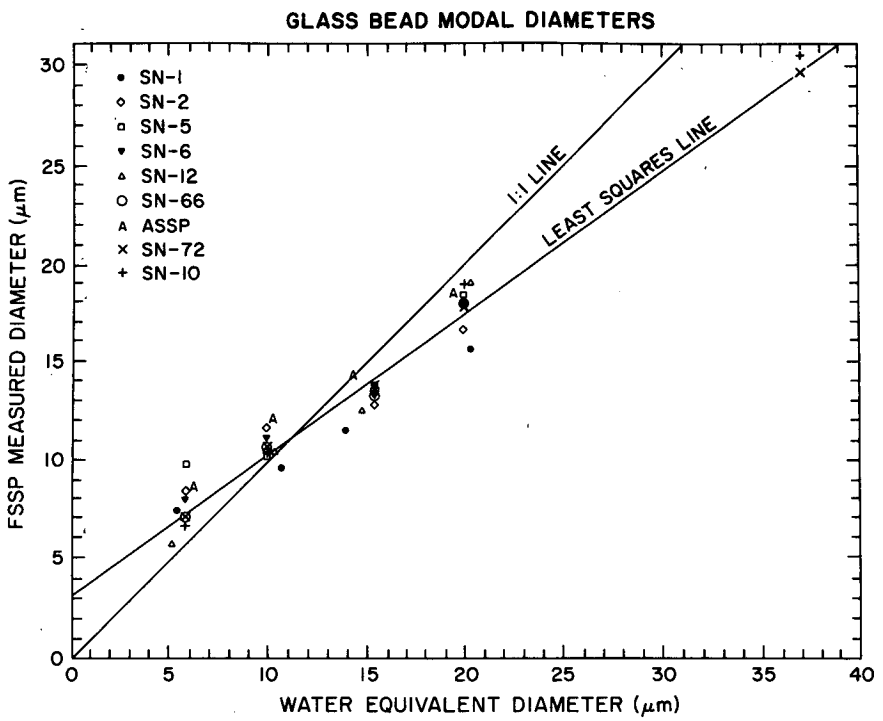

FIG. 3. The FSSP-measured modal diameter of glass bead samples plotted as a function of the water equivalent of the modal diameter. Data from two probes, serial numbers 10 and 72, operating in the 2–47 μm range have been added to the original figure from Dye and Baumgardner (1984) which shows similar data from seven additional probes operating in the 2–30 μm range.

CALIB2 refers to the spectrum obtained by using the linear least-squares glass bead calibration for the FSSP and the manufacturer's calibration for the 2D-GA. With CALIB2, the spectrum comprises the FSSP channels 2–14 and 2D-GA channels 4–62 with a resulting 1.5-μm overlap region. Errors introduced in the LWC calculations by these overlap regions can be as great as 2% in the worst case, but are typically <1%.

Figure 4 shows a comparison of the combined LWC versus particle size spectra using CALIB1 and CALIB2 with data from a worst-case condition in which the maximum LWC is found near the juncture. The total LWCs computed by the two calibrations differ by a factor of 1.7, a fact that is not readily apparent from the figure. The overlapping upper FSSP channels and lower 2D-GA channels that are disregarded during data reduction have been retained here for illustrative purposes. Notice that the lower (and normally disregarded) channels of the 2D-GA significantly undersample the LWC compared to the FSSP in both cases. Recent tests of a 2D cloud probe by Baumgardner (1985) show that glass beads which are correctly sized when dropped through the probe, as was done here, are significantly undersized when passed through the probe at 50 m s^{-1}, which is reasonably close to our experimental conditions of 60 m s^{-1}. These preliminary results also indicate that the sizing error is somewhat dependent upon the particle size and position within the depth-of-field. Since more testing and understanding of this phenomenon are required before these results can be rigorously applied, we have not attempted to apply corrections here, but such corrections would improve agreement between the FSSP and the 2D-GA measurements at the juncture.

5. The mass balance experiment

In this experiment LWCs derived from the KP were compared with those calculated from a knowledge of the rate at which water was emitted from the nozzle and the distribution of this water across the tunnel. The mapping of the LWC profile within the tunnel was performed with the KP itself. Therefore, this technique assumes that for a given droplet spectrum, the KP response to total LWC is linear—it does not matter for this part of the experiment that the KP output may be in error, as long as the error is a constant multiplicative factor. Results in King et al. (1985) show a linear 1:1 response for conditions in which the LWC is ≤ 3 g m^{-3} and the MVD is ≤ 30 μm. We also need to assume that the shape of the drop-size distribution remains substantially constant across the tunnel even though the LWC may vary (otherwise there are possible effects of KP variation with drop size and the problem becomes intractable). It was not possible to check this assumption by sampling, with movable PMS probes, across a

Unauthenticated | Downloaded 06/07/23 02:35 AM UTC

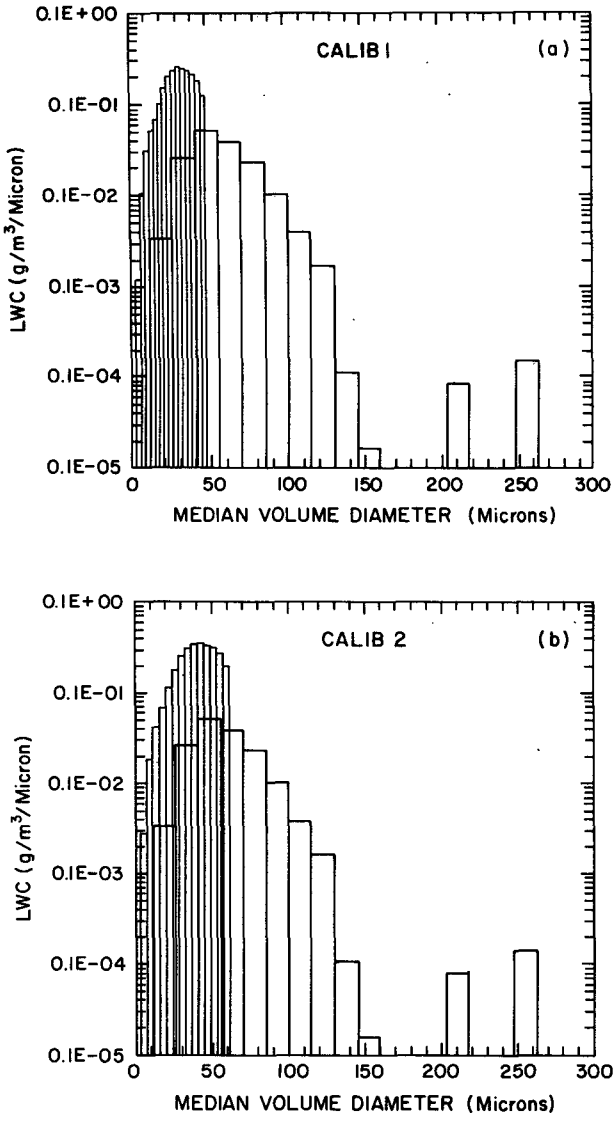

FIG. 4. LWC as a function of drop size using (a) CALIB1 and (b) CALIB2 for data reduction. Using CALIB1, the LWC = 0.74 g m^{-3}, MVD = 33.4 μm, and the dispersion = 0.69; using CALIB2, the LWC = 1.23 g m^{-3}, MVD = 41.4 μm, and the dispersion = 0.83.

stationary spray pattern in the tunnel; however, no significant changes in drop size across the spray pattern were observed when the nozzle, and hence the spray pattern, was moved relative to the fixed location PMS probes.

The water spray in the tunnel was mapped in the horizontal and vertical directions along lines which intersected the center of the sample areas of the KP, FSSP, and 2D-GA probes in their normal positions. A mapping was obtained for each nozzle and for each different pressure setting. In analyzing these maps, the measured points were used to draw isopleths of constant KP output at intervals of either 5% or 10% of the peak value. An example in which isopleths are only drawn at 20% increments for simplicity is shown in Fig. 5. A planimeter was then used to integrate the contribution to the total LWC from each of the annular rings. Using these profiles, the airspeed, and the known water flow rate to the nozzle, these normalized values could then be converted to actual LWCs moving past the sample area. The response of the KP was then determined by comparing the LWC measured by the KP at its normal position to the LWC computed from the profile at that same position.

The data from these intercomparisons have been reduced using both CALIB1 and CALIB2. Figure 6 shows the results using CALIB2. The results obtained using CALIB1 are very similar: the response value for each test is nearly identical and the change in MVD is less than 10 μm. These data indicate that the KP response varies from 100% for drop-size distributions with MVDs of $\approx$20 μm to approximately 50% when the MVD is in the range of 150–200 μm. Although the response curve appears to be nearly linear, there is an indication that the slope is greatest at drop sizes $\leqslant$50 μm and least at the largest drop sizes. In this experiment it was not possible to achieve sprays with 200 μm $\leqslant$ MVDs $\leqslant$ 15 μm. It is presumed that the KP response is 100% for droplet MVDs $\leqslant$ 15 μm assuming allowances are made for collection efficiency.

The LWC could not be held constant throughout this series of experiments and ranged from 0.5 to 2.6 g m^{-3}. While low LWC values are associated with the air atomizing nozzle, the overall LWC values are not distributed in a systematic manner and the shape of the response curve does not appear to be related to the LWC. The correlation coefficient between LWC and MVD is 0.48.

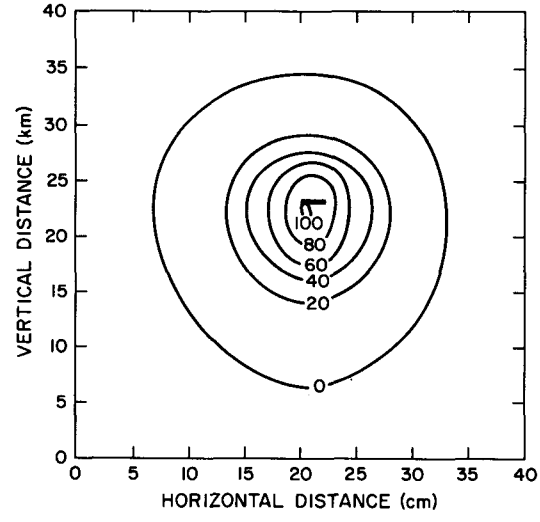

FIG. 5. A map (looking upstream toward the nozzle) of the water spray from a hydraulic nozzle. Isopleths are drawn in terms of the percent of the peak measured value (100% = 1.8 g m^{-3} in this case). The master element of the KP sensor is shown to scale in its normal position.

Unauthenticated | Downloaded 06/07/23 02:35 AM UTC

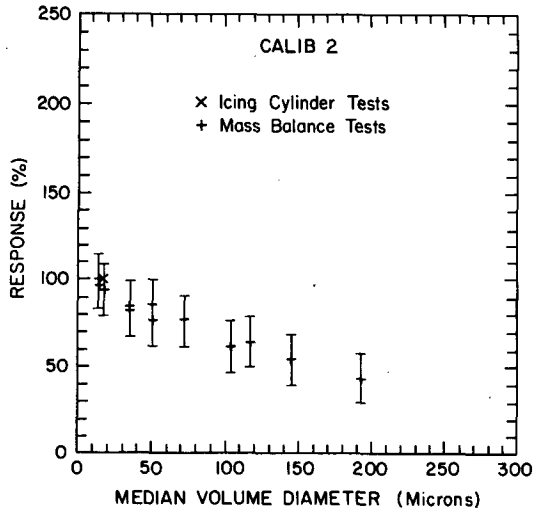

FIG. 6. Response of the KP as a function of drop size using CALIB2. Response is defined as the LWC measured by the KP divided by the LWC computed from the tunnel water profile at the same location. The error bars are discussed in the text.

The X in Fig. 6 represents the average of many tests of the KP in the Canadian National Research Council's (NRC) icing wind tunnel, as reported by King et al. (1985). In those tests a single droplet-size distribution with an MVD of 20 μm and a cutoff of about 30 μm was used. Measurements from the KP were compared with the LWC calculated from the mass of ice accreted on a cylinder during a given time interval. These icing cylinder measurements are thought to be accurate in an absolute sense to better than 10% (Stallabrass, 1978); consequently, the X provides a reasonably accurate independent measure of the KP response at one drop-size distribution. The scatter of the mass-balance data points, particularly the repeated points at $\sim$15, 35 and 50 μm, provides some indication of the relative accuracy and repeatability of the experiment. Potential errors in the component measurements are estimated in the next section.

6. Discussion of errors in the mass-balance experiment

Errors in the mass-balance experiment fall into two general categories: those associated with measuring the LWC with a KP and those associated with determining the LWC within the wind tunnel.

Sources of uncertainty in measurements with a KP are discussed in detail in King et al. (1981). In this application, additional uncertainties arise from minor-amplitude, short-period fluctuations in the strip chart recording which are presumably due to real variations in the LWC. These fluctuations were averaged by using a 30-s sampling period as discussed in section 3. Lesser errors arise from uncertainties in the dimensions of the sensing element and variations in air temperature during a run. When combined, these errors amount to a total of about 5% in the computation of the LWC.

In terms of the values of LWC calculated for the tunnel, there are several potential sources of error. First, the profiling was performed with a sensor that averages over a length of 2 cm. For profiles with widths of the order of this dimension, the resultant smearing causes an underestimate of the peak value of the LWC, and an overestimate in the tail. A quantitative estimate of this effect was obtained by fitting a Gaussian profile to the measured profile, and calculating the smearing errors on the assumption that this was the actual profile. A more thorough approach would be to iterate using this technique a number of times, but since the effect after a single iteration was shown to cause changes in the calculated LWC of less than 5%, it was not pursued further.

The drawing of the isopleths of LWC is another obvious area in which errors could arise in the calculation of the tunnel LWC, particularly as it appears to be a fairly subjective operation. The errors involved in this process were estimated by having two people independently draw the isopleths for the most complex mapping case, and then measuring the total response using the planimeter. (The planimeter itself introduces negligible errors.) The differences between the calculated responses was 3%.

Evaporation of the drops is another major potential source of error in this experiment. The mass flow rate into the nozzles could be obtained within 2% using carefully calibrated flow meters, but any liquid water subsequently evaporated into the air stream would produce the same effect as underreading by the KP. Evaporation of droplets could occur in the tunnel between the nozzle and the sample area as well as in the nozzle housing itself in the case of the air atomizer nozzles. We have not been able to derive any method, either experimental or theoretical, which would enable us to separately estimate the latter effect.

The amount of evaporation in the time it takes for the droplets to move between the nozzle and the sample area has been calculated using a model described in the Appendix. In this model, the drops are accelerated from rest to the tunnel speed in air subsaturated to the upstream value. The subsaturation is assumed constant for the entire trajectory because the amount of LWC evaporated from the drops, even if they were totally evaporated, would have little effect upon the relative humidity since the air is typically so dry—the vapor density deficits are of the order of 8 g m^{-3}, and we were generating total LWCs of about 1 g m^{-3} in the small droplet sprays where evaporation is most critical. The evaporation component of the model is quite standard and largely follows the treatment given in Pruppacher and Klett (1978), although the corrections are larger than might be expected because it takes time for the drops to come up to speed.

The particle acceleration calculations in the model are identical to those described in King (1984). Particle trajectory calculations are by now considered to be

Unauthenticated | Downloaded 06/07/23 02:35 AM UTC

fairly precise, and certainly better than 5%, although in this case one could question the use of steady state drag coefficients for droplets which are experiencing accelerations of the order of 10 g or more. Neglect of the acceleration-dependent drag terms has the effect of underestimating the evaporation because the drops will be calculated to accelerate up to the tunnel speed faster than they might have in reality.

Assuming a typical relative humidity of 30%, the model predicts that up to 28% of the water in the smallest droplet sprays would evaporate before reaching the KP. The veracity of the model was checked by repeating the response tests for three different sprays during a period with an overcast sky and unusually high humidity (86%) conditions. The repeatability of the response values (note the double points at ~15, 35 and 50 μm MVD in Fig. 6) indicate that the combination of absolute errors due to evaporation plus relative errors involved in repeating the tests are less than 10%.

If all the above errors are assumed to be independent, they can be combined in a root-sum-square formulation to yield an overall error of about 13%. This value, which is used for the error bars in Fig. 6, probably overestimates the actual error since the largest contributing component is due to the evaporation error which was estimated from experimental data that inherently contain effects of the other sources of errors.

7. Drop spectrum measurement experiments

In this series of experiments the LWC measured by the KP was compared to the LWC computed from the droplet spectrum comprised of merged data from the PMS FSSP and 2D-GA instruments. These experiments were conducted in two steps. First, the spray was measured simultaneously by the KP and the 2D-GA mounted together in the configuration shown in Fig. 2. These instruments were then replaced by the FSSP, which was mounted on the same pylon. The tunnel was restarted and previous spray conditions were reestablished; measurements were then made with the FSSP.

Since this procedure assumes that the FSSP and the 2D-GA measure the same spray, tests were performed to determine how well the conditions could be repeated. The tunnel and the water spray were started, stabilized at the desired conditions, and then stopped a number of times, and the LWC during the stabilized portion of each cycle was measured with the KP. Tunnel speed could be reset to within 1 m s^{-1}. The standard deviation of the measured LWC was <1%. As mentioned earlier, tests were also conducted to ensure that the KP measurements were not affected by its mounting within the structure of the 2D-GA.

Results from these experiments, using both CALIB1 and CALIB2 for reduction, are shown in Fig. 7. The lack of data points in the interval of approximately 20–40 μm is unfortunate—equipment limitations prevented us from producing stable sprays with these MVDs.

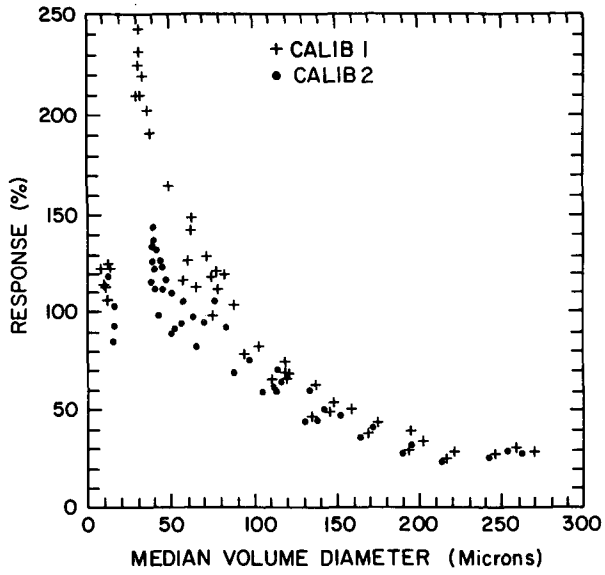

FIG. 7. Response of the KP as computed from the second series of experiments and assuming CALIB1 and CALIB2. Response is defined as the LWC measured by the KP divided by the LWC computed from the merged FSSP and 2D-GA data.

The response curve derived using CALIB1 seems physically meaningless. Performing a detailed error analysis of these data is futile because they are obviously grossly incorrect in an absolute sense. The internal consistency of the data is, however, intriguing, particularly considering that the LWC values are computed from the third moment of the original measurement of the droplet diameter. The fact that these LWC values show a surprisingly small amount of variance suggests that the random instrumental errors are small, indeed. When CALIB2 is used, the resulting response curve is much more reasonable. The difference between the curves strongly suggests that the problem is largely due to incorrect FSSP drop-size calibration techniques.

Figure 8 shows the CALIB2 data points from the drop spectrum tests (the dots in Fig. 7) superimposed on the data points from the mass-balance tests (Fig. 6). The two curves are now in reasonable agreement except near the juncture of the FSSP and 2D-GA data. If the LWC measured by the 2D-GA in channels 4 and 5 is incremented to form a smooth transition between the LWC spectra from the two instruments, the resulting response curve, not shown here, is in complete agreement with that derived from the mass-balance tests. Such an adjustment is not entirely unreasonable since it is obvious (e.g., see Fig. 4) that for whatever reason, the first several channels of the 2D-GA have lower values than the FSSP LWC regardless of the FSSP calibration used. The recent tests by Baumgardner

Unauthenticated | Downloaded 06/07/23 02:35 AM UTC

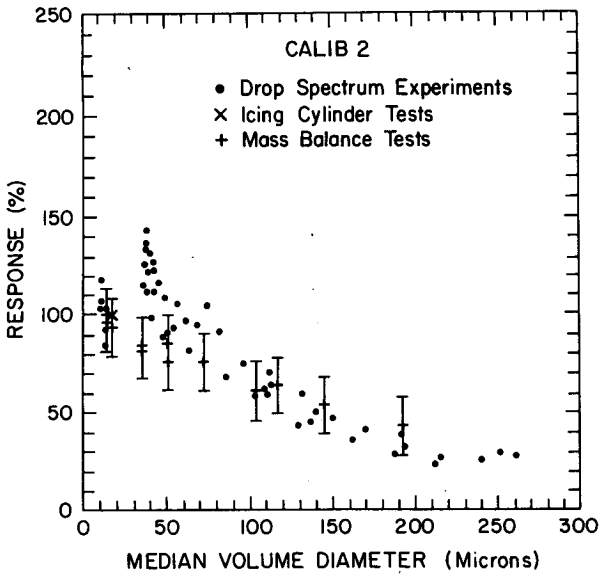

FIG. 8. The response of the KP as a function of drop size as computed from the drop spectrum tests and the mass balance tests.

(1985) indicate one potential reason for such a correction.

8. Summary and conclusions

The response of the King probe liquid water content device to drops of different sizes has been investigated in a wind tunnel. Two series of experiments were conducted: the first compared the probe-measured LWC at different MVDs to the LWC computed through water mass conservation considerations; the second series compared the probe LWC to that computed from the droplet spectra measured by PMS FSSP and 2D-GA probes.

Results from the first series of experiments indicated that, for 60 m s^{-1}, the response decreases in an approximately linear fashion from 100% for a drop-size distribution with an MVD of ~20 μm to about 50% when the MVD is ~150–200 μm. The response to drop sizes outside this range could not be determined due to limitations in the spray equipment.

The response curve derived from the second series of experiments seems physically unreasonable when the manufacturer's calibrations are used to reduce data from the FSSP and 2D-GA probes. These data suggest that the calibration procedures for both these probes, particularly the FSSP, need to be reevaluated. These results, combined with those of Dye and Baumgardner (1984), suggest that the FSSP oversizes drops $\leqslant 11$ μm and undersizes larger ones. The 2D-GA may also be undersizing drops. In addition, measurements from the first few 2D-GA channels (perhaps as high as channel 5, 75 μm, for the probe used) underestimate the mass of water compared to the FSSP regardless of which FSSP calibration is used.

It would be highly desirable to extend this work from 60 m s^{-1} to include the higher aircraft speeds of 80–100 m s^{-1}. We tried to perform the tests at these higher speeds, but even after considerable effort, were unable to maintain a uniform and sufficiently broad spray pattern over a wide range of MVDs at the higher airspeeds. From the results which were obtained, we expect that the KP can be used without correction for measuring the LWC of droplet distribution with the MVDs of less than about 40 μm. As the MVD increases, there will be a gradually diminishing response, which for MVDs of greater than 100 μm will require substantial correction.

Acknowledgments. The investigations described herein were conducted cooperatively by personnel from PMS, CSIRO, and NCAR. We particularly wish to thank PMS for the use of their equipment and facilities, and Darrel Baumgardner (NCAR) for his assistance in bench testing several of the FSSPs. We thank Robert Knollenberg, John Knollenberg, and Dale Hope (PMS), and Darrel Baumgardner and Jack Warner (NCAR) for their valuable consultations. We also thank Brendan Ruiz for his assistance in developing the data reduction program and Walter Grotewold for fabricating numerous components of the test equipment. Frances Huth typed the several versions of this paper.

APPENDIX

Evaporation of Droplets

The LWCs calculated in section 5 on the basis of mass continuity are reliable only so long as evaporation between the nozzle and the test section is accounted for or is negligible. In this Appendix, we present the equations which were used to calculate the evaporation of the drops which were accelerated from rest within the tunnel, in air which was substantially subsaturated (the typical relative humidity was 30%).

To calculate the drop size, a, as a function of time, the following equations were used:

For the change in drop velocity, u,

$$\frac{du}{dt} = \frac{1}{2} C_d \rho_a \pi a^2 (q-u)^2 \tag{A1}$$

where q is the air velocity, ρ_a the density of air, and C_d the drag coefficient, calculated from the Best number Reynolds number relationships of Norment and Zalosh (1974).

For the change in the drop temperature, T_a

$$\frac{dT_a}{dt} = -A(T_a - T_e) + B \tag{A2}$$

where

$$A = 3f[k_a + LD(d\rho_s/dT)]/a^2 c_w \rho_w \tag{A3}$$

and

$$B = 3DLf(1 - \mathrm{RH}/100)\rho_s(T_e)/a^2 c_w \rho_w. \tag{A4}$$

Unauthenticated | Downloaded 06/07/23 02:35 AM UTC

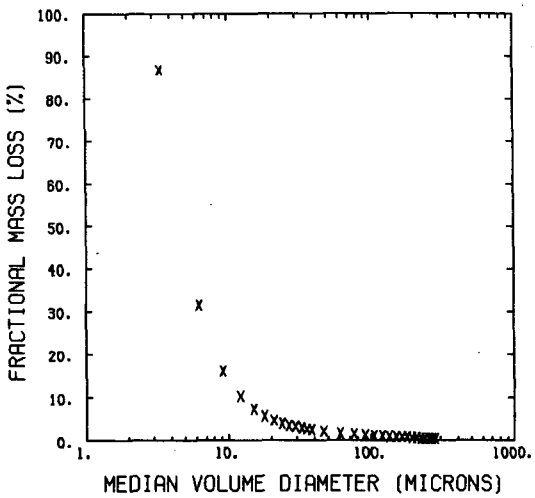

FIG. A1. Fractional mass loss as a function of drop size.

For the ventilation factor, f,

$$f = 1 + 0.086\ \mathrm{Re}, \quad \mathrm{Re} < 2.5$$
$$= 0.78 + 0.275(\mathrm{Re})^{1/2}, \quad \mathrm{Re} \geq 2.5 \quad \text{(A5)}$$

where Re is the Reynolds number.

In (A2) to (A4), T_e is the tunnel air temperature, k_a the thermal conductivity of air, D the thermal diffusivity of water vapor in air, $d\rho_s/dT$ the average rate of change of saturated vapor density over water with temperature in the range between T_a and T_e, ρ_w, and c_w are the density and specific heat of water, respectively, and RH is the relative humidity.

For the mass loss

$$a\frac{da}{dt} = -Df[\rho_s(T_a) - \rho(T_e)]/\rho_w. \quad \text{(A6)}$$

The ventilation, heat and mass balance equations are those given by Pruppacher and Klett (1978).

This set of differential equations was solved numerically with the following parameters: pressure is 84 kpa, T_e is 8°C, RH is 30%, initial drop temperature is 20°C, distance from nozzle to probe is 0.94 m, and air velocity is 60 m s^{-1}. The fractional mass loss as a function of size is presented in Fig. A1. As expected, the fractional mass loss is greatest for the smallest drops, but for drops greater than 40-μm diameter the size effect is less pronounced than one would intuitively expect because the large drops, which usually suffer negligible evaporation, take longer to come up to the tunnel speed because of their inertia, and are consequently ventilated at higher rates for longer times. When these evaporation effects are applied to the drop-size spectra used in the tests, the overall correction amounts to 28% in the worst-case.

REFERENCES

Barrett, E. W., 1958: A comparative flight test of three instruments for measuring cloud water content. Tech. Note No. 14, Cloud Physics Laboratory, University of Chicago, 17 pp.

Baumgardner, D., 1985: Particle size calibrations of two optical array probes. *Newsletter on Developments of Airborne Cloud Physics Instruments,* June 1985, NCAR, 1–3.

——, J. W. Strapp and J. E. Dye, 1985: Evaluation of the Forward Scattering Spectrometer Probe. Part II: Corrections for coincidence and dead-time losses. *J. Atmos. Oceanic Technol.,* **2,** 626–632.

Cerni, T. A., 1983: Determination of the size and concentration of cloud drops with an FSSP. *J. Climate Appl. Meteor.,* **22,** 1346–1355.

Cooper, W. A., 1978: Cloud physics investigations by the University of Wyoming in HIPLEX 1977. Report No. AS119, University of Wyoming, 320 pp.

Dye, J. E., and D. Baumgardner, 1984: Evaluation of the Forward Scattering Spectrometer Probe. Part I: Electronic and optical studies. *J. Atmos. Oceanic Technol.,* **1,** 329–344.

King, W. D., 1982: Comparison of FSSP and CSIRO liquid water probes. *Cloud Particle Measurement Symposium: Summaries and Abstracts,* NCAR/TN-199+PROC, NCAR, 41–43.

——, 1984: Air flow and particle trajectories around aircraft fuselages. I: Theory. *J. Atmos. Oceanic Technol.,* **1,** 5–13.

——, C. T. Maher and G. A. Hepburn, 1981: Further performance tests on the CSIRO liquid water probe. *J. Appl. Meteor.,* **20,** 195–202.

——, J. E. Dye, J. W. Strapp, D. Baumgardner and D. Huffman, 1985: Icing wind tunnel tests on the CSIRO liquid water probe. *J. Atmos. Oceanic Technol.,* **2,** 293–303.

Knollenberg, R. E., 1970: The optical array: An alternative to scattering or extinction for airborne particle size determination. *J. Appl. Meteor.,* **9,** 86–103.

——, 1972: Comparative liquid water content measurements of conventional instruments with an optical array spectrometer. *J. Appl. Meteor.,* **11,** 501–508.

Norment, H. G., and R. G. Zalosh, 1974: Effects of airplane flow fields on hydrometeor concentration measurements. AFCRL-TR-74-0602, Air Force Cambridge Research Lab, 101 pp.

Owens, G. V., 1975: Wind tunnel calibrations of three instruments designed for measurements of the liquid water content of clouds. Tech. Note 10, Cloud Physics Laboratory, the University of Chicago, 15 pp.

Pruppacher, H. R., and J. D. Klett, 1978: *Microphysics of Clouds and Precipitation.* D. Reidel, 714 pp.

Stallabrass, J., 1978: An appraisal of the single rotating cylinder method of liquid water content measurement. Tech. Note LTR-LT-92, National Research Council, Canada, 40 pp.

Unauthenticated | Downloaded 06/07/23 02:35 AM UTC